OXFORD

SOT | Society of Toxicology

www.toxsci.oxfordjournals.org

TOXICOLOGICAL SCIENCES, 168(2), 2019, 365–380

doi: 10.1093/toxsci/kfy299

Advance Access Publication Date: December 18, 2018

Research Article

Evaluation of Possible Proarrhythmic Potency: Comparison of the Effect of Dofetilide, Cisapride, Sotalol, Terfenadine, and Verapamil on hERG and Native I_{Kr} Currents and on Cardiac Action Potential

Péter Orvos,[*,†,1] Zsófia Kohajda,[*,‡,1] Jozefina Szlovák,[*] Péter Gazdag,[*] Tamás Árpádffy-Lovas,[*] Dániel Tóth,[*] Amir Geramipour,[*] László Tálosi,[§] Norbert Jost,[*,‡,¶] András Varró,[*,‡,¶,2] and László Virág[*,‡,¶]

[*]Department of Pharmacology and Pharmacotherapy, Faculty of Medicine; [†]Department of Ophthalmology, University of Szeged, Szeged H-6720, Hungary; [‡]MTA-SZTE Research Group for Cardiovascular Pharmacology, Hungarian Academy of Sciences, Szeged H-6720, Hungary; [§]Department of Pharmacognosy, Faculty of Pharmacy; and [¶]Department of Pharmacology and Pharmacotherapy, Interdisciplinary Excellence Centre, University of Szeged, Szeged H-6720, Hungary

[1]These authors contributed equally to this study.

[2]To whom correspondence should be addressed at Department of Pharmacology and Pharmacotherapy, Faculty of Medicine, University of Szeged, Dóm tér 12, Szeged H-6720, Hungary. Fax: +36-62-545-682. E-mail: varro.andras@med.u-szeged.hu.

The authors certify that all research involving human subjects was done under full compliance with all government policies and the Helsinki Declaration.

ABSTRACT

The proarrhythmic potency of drugs is usually attributed to the I_{Kr} current block. During safety pharmacology testing analysis of I_{Kr} in cardiomyocytes was replaced by *human ether-a-go-go-related gene* (hERG) test using automated patch-clamp systems in stable transfected cell lines. Aim of this study was to compare the effect of proarrhythmic compounds on hERG and I_{Kr} currents and on cardiac action potential. The hERG current was measured by using both automated and manual patch-clamp methods on HEK293 cells. The native ion currents (I_{Kr}, I_{NaL}, I_{CaL}) were recorded from rabbit ventricular myocytes by manual patch-clamp technique. Action potentials in rabbit ventricular muscle and undiseased human donor hearts were studied by conventional microelectrode technique. Dofetilide, cisapride, sotalol, terfenadine, and verapamil blocked hERG channels at 37°C with an IC_{50} of 7 nM, 18 nM, 343 μM, 165 nM, and 214 nM, respectively. Using manual patch-clamp, the IC_{50} values of sotalol and terfenadine were 78 μM and 31 nM, respectively. The IC_{50} values calculated from I_{Kr} measurements at 37°C were 13 nM, 26 nM, 52 μM, 54 nM, and 268 nM, respectively. Cisapride, dofetilide, and sotalol excessively lengthened, terfenadine, and verapamil did not influence the action potential duration. Terfenadine significantly inhibited I_{NaL} and moderately I_{CaL}, verapamil blocked only I_{CaL}. Automated hERG assays may over/underestimate proarrhythmic risk. Manual patch-clamp has substantially higher sensitivity to certain drugs. Action potential studies are also required to analyze complex multichannel effects. Therefore, manual patch-clamp and action potential experiments should be a part of preclinical safety tests.

Key words: safety pharmacology; proarrhythmia; hERG; I_{Kr}; cardiac action potential.

Life threatening cardiac arrhythmias and sudden cardiac death caused by drugs are one of the major safety issues for pharmaceutical industry and regulatory agencies (Polonchuk, 2012). In the past, several drugs such as cisapride, grepafloxacin, terfenadine, and terodiline have been withdrawn from major markets because of their proarrhythmic effect (Hishigaki and Kuhara, 2011; Varró and Baczkó, 2011). The therapeutic use of these agents, in the worst case, has led to ventricular fibrillation-induced cardiac arrest and consequently sudden cardiac death. Furthermore, drug withdrawn from the market is particularly costly and may harm the prestige of the company as well (Farre *et al.*, 2007).

Many of drugs and potential drug candidate molecules exert their arrhythmogenic effects through the $K_v11.1$ voltage-gated potassium ion channel encoded by the *human ether-a-go-go-related gene* (hERG, KCNH2) (Alexander *et al.*, 2011). This pore-forming protein expressed in ventricular cardiocytes, and represents the α-subunit of the ion channel responsible for rapid delayed rectifier potassium current (I_{Kr}) (Sanguinetti *et al.*, 1995; Trudeau *et al.*, 1995). hERG channel has been found extremely promiscuous in its interactions with a wide range of pharmacological entities (Farre *et al.*, 2007). The I_{Kr} current plays a fundamental role in the phase 3 of repolarization of the action potential; therefore, inhibition of hERG channel delays cardiac action potential repolarization, which lengthens the action potential duration (APD). The drug-induced repolarization delay might associate with catastrophic polymorphic ventricular tachycardia (torsades de pointes, TdP). This mechanism is the basis of fatal ventricular fibrillation and sudden death (Hancox *et al.*, 2008; Lengyel *et al.*, 2007; Yap and Camm, 2003). Based on this concept investigation of I_{Kr} blocking and action potential repolarization duration lengthening capabilities became of required item of safety pharmacology profile of drugs. At present, to avoid severe cardiotoxicity, every new compound is to go through preclinical safety testing determined by the U.S. Food and Drug Administration, the European Medicines Agency and other regulatory entities. Preclinical studies have to be carried out according to the International Conference on Harmonization's S7B guideline. *In vitro* electrophysiological experiments require on cardiac action potential and/or cardiac ionic currents, whereas *in vivo* studies can directly demonstrate the drug-induced QT interval prolongation.

Among the *in vitro* assays, repolarization lengthening effect of the investigational compounds can be adequately analyzed with conventional microelectrode technique in different cardiac structures such as Purkinje fibers and papillary muscles. This method allows the direct observation the alterations of cardiac action potential waveform in cellular level, but gives no specific information about the currents pass through different types of ion channels (Hodgkin and Huxley, 1945). Today, ion channel function and transmembrane ionic currents such as I_{Kr} are most precisely studied using the conventional manual patch-clamp technique (Neher and Sakmann, 1976; Neher *et al.*, 1978). By this method, measurement of the activity of individual channels or the entire ion channel population of the cell is routinely achievable. This technique has become the "gold standard" in studying ion channel behavior, function, kinetics, and pharmacology, mainly in native mammalian cells (Dabrowski *et al.*, 2008; Dunlop *et al.*, 2008; Farre and Fertig, 2012; Farre *et al.*, 2007, 2008; Fertig *et al.*, 2002). The conventional microelectrode technique and the manual patch-clamp method offer direct, information-rich, and real-time *in vitro* technologies to study proarrhythmic effect of drugs and drug candidate compounds. Although providing excellent data quality, these tests are complicated, time consuming and expensive for the large numbers of compounds before the extensive pharmacodynamic experiments can be initiated, because they require the continuous presence of highly skilled and trained personnel. Therefore, these problems excludes the aforementioned techniques as screening tools in early drug development and optimization (Dabrowski *et al.*, 2008; Dunlop *et al.*, 2008; Farre and Fertig, 2012; Farre *et al.*, 2007, 2009). In recent years, numerous companies have developed and introduced automated patch-clamp platforms for high-throughput screening, which are mainly used with stably expressing cell lines and suitable for rapid and high quality optimization of drug candidates. The breakthrough in automated electrophysiology came when planar patch-clamp method without micromanipulation or visual control was launched (Fertig *et al.*, 2002; Lü and An, 2008). This innovative technology facilitates functional data on ion channel active compounds with the throughput capability that is significantly higher compared with conventional techniques (Dunlop *et al.*, 2008; Farre and Fertig, 2012; Farre *et al.*, 2007, 2009). Therefore, analysis of I_{Kr} current in heart muscle cells was typically replaced by the examination of its recombinant equivalent hERG current using automated patch-clamp systems and stable transfected cell lines.

However, more and more evidence indicates that the different proarrhythmic pharmacological assays result in contradictory outcomes raising serious questions regarding their predictability for *in vivo* situations including clinical settings. Assays often give false-positive and -negative results or over/underestimate the cardiac proarrhythmic effect. Therefore, aim of this study was to compare the effect of different known proarrhythmic compounds on hERG and I_{Kr} currents and on cardiac action potential to determine the value of *in vitro* assays in evaluation of cardiac proarrhythmic risk of these compounds and help to understand the nature of proarrhythmic pharmacological safety drug tests.

MATERIALS AND METHODS

Chemicals

All chemicals, which are not specifically indicated, were purchased from Sigma-Aldrich Ltd (Budapest, Hungary). To study the effect of dofetilide, cisapride monohydrate, terfenadine, and verapamil, stock solutions were prepared from these compounds, where the concentrations were 10 mM and the solubilizing agent was dimethyl sulfoxide (DMSO). Aliquots were stored at −20°C for up to 2–4 weeks. (±)-Sotalol hydrochloride was acquired from Sequoia Research Products Ltd (Pangbourne, UK). Sotalol was dissolved directly in external solution at 10 mM concentration before experiments. For electrophysiological measurements, stock solutions were further diluted with external solution, to give appropriate concentrations for the patch-clamp experiments. The final DMSO concentrations in the tested samples were 1% or less.

Ethics Statement and Species

Patients. Hearts were obtained from organ donors whose nondiseased hearts were explanted to obtain pulmonary and aortic valves for transplant surgery. Before cardiac explantation, organ donors did not receive medication apart from dobutamine, furosemide, and plasma expanders. The investigations conformed to the principles of the *Declaration of Helsinki*. Experimental protocols were approved by the National Scientific and Research Ethical Review Boards (4991-0/2010-1018EKU [339/PI/010]).

Animals. All experiments were carried out in compliance with the *Guide for the Care and Use of Laboratory Animals* (USA NIH publication NO 85-23, revised 1996) and conformed to the Directive 2010/63/EU of the European Parliament. The protocols have been approved by the Ethical Committee for the Protection of Animals in Research of the University of Szeged, Szeged, Hungary (approval number: I-74-5-2012) and by the Department of Animal Health and Food Control of the Ministry of Agriculture and Rural Development (authority approval number XIII/1211/2012).

Conventional Microelectrode Technique

Action potentials were recorded in ventricular trabeculae and papillary muscle preparations obtained from the right ventricles of rabbit or from undiseased human donor hearts using conventional microelectrode techniques. New Zealand rabbits of either sex weighing 2–3 kg were sacrificed by cervical dislocation after an intravenous injection of 400 U/kg heparin. Then the chest was opened, and the heart was rapidly removed. The heart was immediately rinsed in oxygenated modified Locke's solution containing (in mM): NaCl 128.3, KCl 4, $CaCl_2$ 1.8, $MgCl_2$ 0.42, $NaHCO_3$ 21.4, and glucose 10. The pH of this solution was set between 7.35 and 7.4 when gassed with the mixture of 95% O_2 and 5% CO_2 at 37°C. In case of human donor hearts, after explantation, each heart was perfused with cardioplegic solution and kept cold (4–6°C) for 2–4 h before dissection.

Isolated muscle preparations obtained from the right ventricle were individually mounted in a tissue chamber with the volume of 50 ml. Each preparation was initially stimulated through a pair of platinum electrodes in contact with the preparation using rectangular current pulses of 2 ms duration. These stimuli were delivered at a constant cycle length of 1000 ms for at least 60 min allowing the preparation to equilibrate before the measurements were initiated. Transmembrane potentials were recorded using conventional glass microelectrodes, filled with 3 M KCl and having tip resistances of 5–20 MΩ, connected to the input of a high impedance electrometer (Experimetria, type 309, Budapest, Hungary) which was coupled to a dual beam oscilloscope. The resting potential (RP), action potential amplitude (APA), maximum upstroke velocity (V_{max}), and APD measured at 50% and 90% of repolarization (APD_{50} and APD_{90}, respectively) were off-line determined using a home-made software (APES) running on a computer equipped with an ADA 3300 analog-to-digital data acquisition board (Real Time Devices, Inc., State College, Pennsylvania) having a maximum sampling frequency of 40 kHz. Stimulation with a constant cycle length of 1000 ms was applied in the course of all experiments. Attempts were made to maintain the same impalement throughout each experiment. In case an impalement became dislodged, adjustment was attempted, and if the action potential characteristics of the re-established impalement deviated by less than 5% from the previous measurement, the experiment continued (Jost *et al.*, 2005; Kristóf *et al.*, 2012; Lengyel *et al.*, 2001; Orvos *et al.*, 2015). All measurements were carried out at 37°C.

Conventional Manual Patch-clamp Measurements

Left ventricular myocytes were enzymatically dissociated from hearts of New Zealand rabbits of either sex weighing 2–3 kg using the retrograde perfusion technique. The chest is opened and the heart is quickly removed and placed into cold (4–8°C) solution with the following composition (in mM): NaCl 135, KCl 4.7, KH_2PO_4 1.2, $MgSO_4$ 1.2, HEPES 10, $NaHCO_3$ 4.4, Glucose 10, $CaCl_2$ 1 (pH 7.2). The heart is then mounted on a modified, 60 cm high Langendorff column and perfused with oxygenated perfusate of the same composition warmed to 37°C. After 3–5 min of perfusion to flush blood from the coronary vasculature, the perfusate is switched to one having no exogenously added calcium (ie, to one that is nominally Ca^{2+}-free) until the heart cease contracting (~8 to 10 min). Enzymatic digestion is accomplished by perfusion with the same, nominally Ca^{2+}-free solution with 260 U/ml Collagenase (Worthington Type 2) and 33 μM $CaCl_2$. After 10–15 min the heart is removed from the aortic cannula and placed into enzyme free solution containing 1 mM $CaCl_2$ warmed to 37°C for 15 min. Then, the tissue is minced into small chunks, and following gentle agitation myocytes are separated by filtering the resulting slurry through a nylon mesh. Myocytes are finally harvested by gravity sedimentation. Once the majority of individual myocytes has settled to the bottom of the container, the supernatant is decanted and replaced with Tyrode's solution and the myocytes are resuspended by gentle agitation. This procedure is repeated twice more and the resulting myocyte suspension is stored in HEPES buffered Tyrode's solution at room temperature.

One drop of cell suspension was placed in a transparent recording chamber mounted on the stage of an inverted microscope. The myocytes were allowed to settle and adhere to the bottom for at least 5–10 min before superfusion was initiated with Tyrode solution containing (in mM): NaCl 144, NaH_2PO_4 0.4, KCl 4.0, $CaCl_2$ 1.8, $MgSO_4$ 0.53, glucose 5.5, and HEPES 5.0 (pH 7.4, NaOH). Temperature was set to 37°C. Only rod-shaped cells with clear cross-striations were used. Patch-clamp micropipettes were fabricated from borosilicate glass capillaries using a micropipette puller (Flaming/Brown, type P-97, Sutter Co, Novato, California). These electrodes had resistances between 1.5 and 2.5 MΩ. Membrane currents were recorded with Axopatch 200B patch-clamp amplifiers (Molecular Devices, Inc., Sunnyvale, California) using the whole-cell configuration of the patch-clamp technique. After establishing a high resistance (1–10 GΩ) seal by gentle suction, the cell membrane beneath the tip of the electrode was disrupted by suction or application of short electrical pulses. Membrane currents were digitized after low-pass filtering at 1 kHz using analog-to-digital converters (Digidata 1440 A, Molecular Devices, Inc.) under software control (pClamp 10, Molecular Devices, Inc.). The same software was used for off-line analysis (Kristóf *et al.*, 2012).

When measuring rapid delayed rectifier potassium currents (I_{Kr}), pipette solution was contained (in mM): KOH 110, KCl 40, K_2ATP 5, $MgCl_2$ 5, EGTA 5, HEPES 10 (pH was adjusted to 7.2 by aspartic acid). Nisoldipine (1 μM) was added to the external solution to eliminate L-type Ca^{2+} current (I_{CaL}). The slow component of the delayed rectifier potassium current (I_{Ks}) was inhibited by using the selective I_{Ks} blocker HMR 1556 (0.5 μM). I_{Kr} was activated by 1000 ms long depolarizing voltage pulses with the pulse frequency of 0.05 Hz to the test potential of 20 mV and then the cell was repolarized to −40 mV. The deactivating tail current at −40 mV after the test pulse was assessed as I_{Kr}. The amplitudes of the I_{Kr} tail currents were determined as the difference between the peak tail current and the baseline (Lengyel *et al.*, 2001). Before the depolarizing test pulse 500 ms long prepulse to −40 mV was applied to ensure the baseline region. The holding potential was −80 mV. After control period, maximum 2 increasing concentrations of the test compound were applied, each for approximately 6–8 min (in case of dofetilide 10 min). Unlike during I_{Kr} measurements in native myocytes, the solutions and the voltage protocol for manual patch-clamp experiments on HEK-hERG cell line were the same as used during automated patch-clamp experiments (see below).

The L-type calcium current (I_{CaL}) was recorded in HEPES-buffered Tyrode's solution supplemented with 3 mM 4-aminopyridine. A special solution was used to fill the micropipettes (composition in mM: CsCl 125, TEACl 20, MgATP 5, EGTA 10, HEPES 10, pH was adjusted to 7.2 by CsOH). I_{CaL} was evoked by 400 ms long depolarizing voltage pulses to various test potentials ranging from −35 to 40 mV. The holding potential was −80 mV. A short prepulse of −40 mV served to inactivate Na^+ current. The amplitude of the I_{CaL} was defined as the difference between the peak inward current at the beginning of the pulse and the current at the end of the pulse (Jost *et al.*, 2013).

The late sodium current (I_{NaL}) was activated by depolarizing voltage pulses to −20 mV from the holding potential of −120 mV. After 5–7 min incubation with terfenadine the external solution was replaced by that containing 20 μM tetrodotoxin (TTX). TTX at this concentration completely blocks the late sodium current. The external solution was HEPES-buffered Tyrode's solution supplemented with 1 μM nisoldipine, 0.5 μM HMR-1556, and 0.1 μM dofetilide to block I_{CaL}, I_{Ks}, and I_{Kr} currents. The composition of the pipette solution (in mM) was: KOH 110, KCl 40, K_2ATP 5, $MgCl_2$ 5, EGTA 5, HEPES 10 (pH was adjusted to 7.2 by aspartic acid) (Kohajda *et al.*, 2016).

Automated Planar Patch-clamp Measurements

The hERG channel current was measured by using planar patch-clamp technology in the whole-cell configuration with a 4 channel medium-throughput fully automated patch-clamp platform (Patchliner Quattro, Nanion Technologies GmbH, Munich, Germany) with integrated temperature control. Data acquisition and online analysis were performed with an EPC-10 Quadro patch-clamp amplifier (HEKA Elektronik Dr Schulze GmbH, Lambrecht/Pfalz, Germany), using PatchMaster 2.65 software (HEKA Elektronik Dr. Schulze GmbH). The pipetting protocols were controlled by PatchControlHT 1.09.30 software (Nanion Technologies GmbH).

Experiments were carried out at room or physiological (37°C) temperature, on HEK293 (human embryonic kidney) cells stably expressing the hERG (Kv11.1) potassium channel. The cell line originated from Cell Culture Service GmbH (Hamburg, Germany). Cells were cultured at 37°C, in 5% CO_2 in IMDM medium (PAA Laboratories GmbH, Pasching, Austria) supplemented with 10% FBS (PAA Laboratories GmbH), 2 mM L-glutamine (Life Technologies Corporation, Carlsbad, California), 1 mM Na-piruvate (PAA Laboratories GmbH), and 500 μg/ml G418 (PAA Laboratories GmbH). Suspension of cells was used for measurements from running cell culture. Cells were washed twice with PBS (Life Technologies Corporation) and then detached with trypsin-EDTA (PAA Laboratories GmbH) for 30–60 s before the measurement. Trypsin was blocked with the serum-containing medium. The cell suspension was next centrifuged (2 min, 100 × g), resuspended in IMDM medium at a final density of 1×10^6–5×10^6 cells/ml, and kept in the cell hotel of the Patchliner. Cells were recovered after 15–30 min and remained suitable for automated patch-clamp recordings for up to 4 h.

The following solutions were used during patch-clamp recording (compositions in mM): internal solution: KCl 50, NaCl 10, KF 60, EGTA 20, HEPES 10, pH 7.2 (KOH); external solution: NaCl 140, KCl 4, glucose-monohydrate 5, $MgCl_2$ 1, $CaCl_2$ 3, HEPES 10, pH 7.4 (NaOH). All solutions were sterile filtered. Aliquots were stored at −20°C and warmed up to room temperature before use. The voltage protocol for hERG ion channel started with a short (100 ms) −40 mV step to establish the baseline region. A depolarizing step was applied to the test potential of 20 mV for 3 s, and then the cell was repolarized to −40 mV to evoke outward tail current. Holding potential was −80 mV. The pulse frequency was approximately 0.1 Hz. Currents were low-pass filtered at 2.9 kHz using the internal Bessel filter of the EPC-10 Quadro patch-clamp amplifier (HEKA Elektronik Dr. Schulze GmbH) and digitized at 10 kHz. The peak tail current was corrected the leak current defined during the first period to −40 mV. Recording started in external solution. After this control period, 6 increasing concentrations of the test compound were applied, each for approximately 3 min (in case of dofetilide 6 min) to record a complete concentration-response curve. Amitriptyline (10 μM) was applied as a reference inhibitor then a wash-out step terminated the protocol.

Statistics

All data are expressed as means ± SEM. The "*n*" number refers to the number of experiments (ie, the number of cells in case of patch-clamp and the number of ventricular muscle preparations—papillary or trabecular muscle—in case of action potential measurements) except native I_{Kr} measurements when it refers to the number of experiments regarding 1 data point of the concentration-response curve and the means ± SEM values were calculated accordingly. Statistical analysis was performed with Student's *t* test for paired data or one-way analysis of variance (ANOVA). The results were considered statistically significant when p was $<.05$.

RESULTS

All compounds (dofetilide, cisapride, sotalol, terfenadine, and verapamil) were tested in hERG assay at both room temperature and 37°C with automated patch-clamp system. The elevation of ambient temperature to physiologic significantly altered the characteristic of hERG current. The current density of peak tail current increased from 21.97 ± 0.40 pA/pF to 32.42 ± 0.69 pA/pF ($n = 19$–24, $p < .05$). The rise time of tail current was decreased and the time constant of decay phase was more rapid (tau changed from 761.52 ± 16.77 ms to 394.15 ± 8.69 ms, $n = 19$–23, $p < .05$).

All investigated compounds inhibited the hERG current at both temperatures. The IC_{50} values of the dofetilide elicited inhibition were very similar (8.4 ± 0.2 nM, $n = 6$ at room temperature and 7.3 ± 0.2 nM, $n = 5$ at 37°C). The other compounds displayed different properties at room temperature versus physiological temperature (37°C). Cisapride, sotalol, terfenadine, and verapamil blocked hERG channels at room temperature with an IC_{50} of 47.5 ± 4.8 nM, $n = 5$; 773.7 ± 9.3 μM, $n = 5$; 266.0 ± 26.8 nM, $n = 6$; and 344.9 ± 26.1 nM, $n = 5$, respectively. However, at 37°C these compounds found to be much more potent (IC_{50} values were 17.7 ± 2.9 nM, $n = 5$; 342.8 ± 24.8 μM, $n = 5$; 165.4 ± 24.5 nM, $n = 6$; and 213.6 ± 22.5 nM, $n = 5$, respectively).

To evaluate the prognostic value of hERG assay these agents were subjected for further investigations. The I_{Kr} current blocking capability of the compounds was tested on rabbit ventricular myocytes with manual patch-clamp method at 37°C. The corresponding IC_{50} values of dofetilide, cisapride, and verapamil were 13.0 ± 2.6 nM ($n = 3$–4), 26.4 ± 4.5 nM ($n = 3$–5), and 268.2 ± 11.2 nM ($n = 4$–5), respectively, showing a good correlation with IC_{50} values obtained in hERG assays. On the contrary, IC_{50} values derived from I_{Kr} measurements was approximately 7 and 3 times lower (51.6 ± 8.8 μM, $n = 2$–6 and 54.3 ± 5.2 nM, $n = 3$–4, respectively) in case of sotalol and terfenadine. The results of both automated and manual patch-clamp experiments are shown in Figures 1–5 and Table 1.

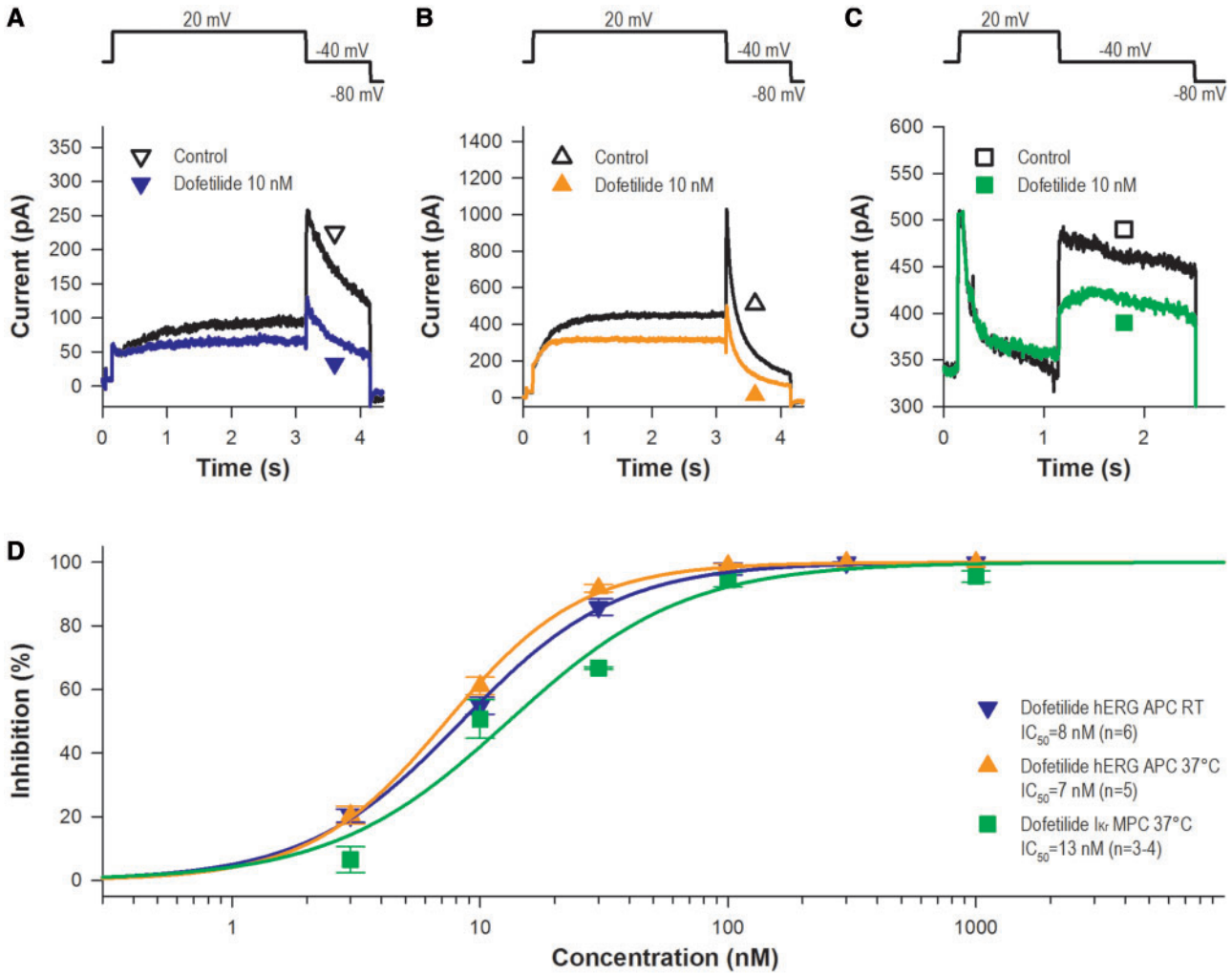

Figure 1. Effect of dofetilide on hERG and I_{Kr} current. A, Example traces for hERG mediated currents obtained from HEK-hERG cell treated with 10 nM dofetilide at room temperature (RT). B, Effect of 10 nM dofetilide on hERG current at 37°C. C, Sample I_{Kr} current sweeps obtained from rabbit left ventricular muscle cell treated with 10 nM dofetilide. The currents were recorded using the voltage protocols shown at the top of panels (A–C). D, Dose-response curves of dofetilide derived from hERG measurements at RT and at 37°C and from I_{Kr} experiments. Abbreviations: APC, automated patch-clamp; MPC, manual patch-clamp.

As sotalol and terfenadine have stronger effect on I_{Kr} measured by manual patch-clamp method compared with hERG automated patch-clamp experiments, the effects of these drugs on hERG current using manual patch-clamp technique at 37°C were also investigated to study how the potency of these drugs are influenced by the experimental techniques themselves. In contrast with the hERG automated patch-clamp assays, the effects of sotalol and terfenadine on hERG current were stronger measured by the manual patch-clamp technique: IC_{50} values calculated from the hERG manual patch-clamp experiments were 77.5 ± 4.8 μM (n = 3–7) and 31.0 ± 3.2 nM (n = 3–5), respectively, showing still somewhat different but far less discrepancy with the native I_{Kr} measurements (Figs. 3 and 4).

To study the safety pharmacology consequences of the hERG and I_{Kr} inhibition of dofetilide, cisapride, sotalol, terfenadine, and verapamil, the effect of these compounds on action potential configuration was studied in rabbit right ventricular papillary muscle preparations. In these investigations, the IC_{50} concentrations obtained from I_{Kr} experiments were applied. Dofetilide, cisapride, and sotalol significantly lengthened the APD at stimulation cycle length of 1000 ms. The prolongation of APD_{90} was 47.8 ± 12.9% (n = 7) in case of 13 nM dofetilide, 68.4 ± 10.0% (n = 6) in case of 26 nM cisapride, whereas 52 μM sotalol extended the APD with 56.0 ± 4.6% (n = 5). Verifying by one-way ANOVA these APD lengthenings were not significantly different. In contrast, terfenadine (1.4 ± 3.0%, n = 8) and verapamil (0.6 ± 1.8%, n = 5) did not significantly affect the APD at 54 and 270 nM concentrations, respectively (Figure 6 and Table 2).

As terfenadine and verapamil did not influence the action potential repolarization, the possible effects of these compounds on the late Na^+ current (I_{NaL}) and on the L-type inward calcium current (I_{CaL}) were also investigated in rabbit ventricular myocytes. These experiments clearly revealed that terfenadine at 54 nM concentration significantly inhibited I_{NaL} (Figure 7, from 82.8 ± 17.9 pA to 45.8 ± 7.9 pA, n = 4, $p < .05$ at −20 mV test potential). A slight but significant block on I_{CaL} by 54 nM terfenadine was also observed (Figure 8). Verapamil at 270 nM did not influenced the I_{NaL} current (control: 56.5 ± 11.2 pA, drug: 49.0 ± 9.2 pA, n = 4, not significant, see Figure 7), whereas a moderate but significant inhibition of I_{CaL} current was observed after application of 270 nM verapamil (Figure 8).

In purpose to confirm our findings in rabbit ventricular myocytes, effect of dofetilide, cisapride, sotalol, terfenadine, and verapamil were also studied on action potential repolarization in

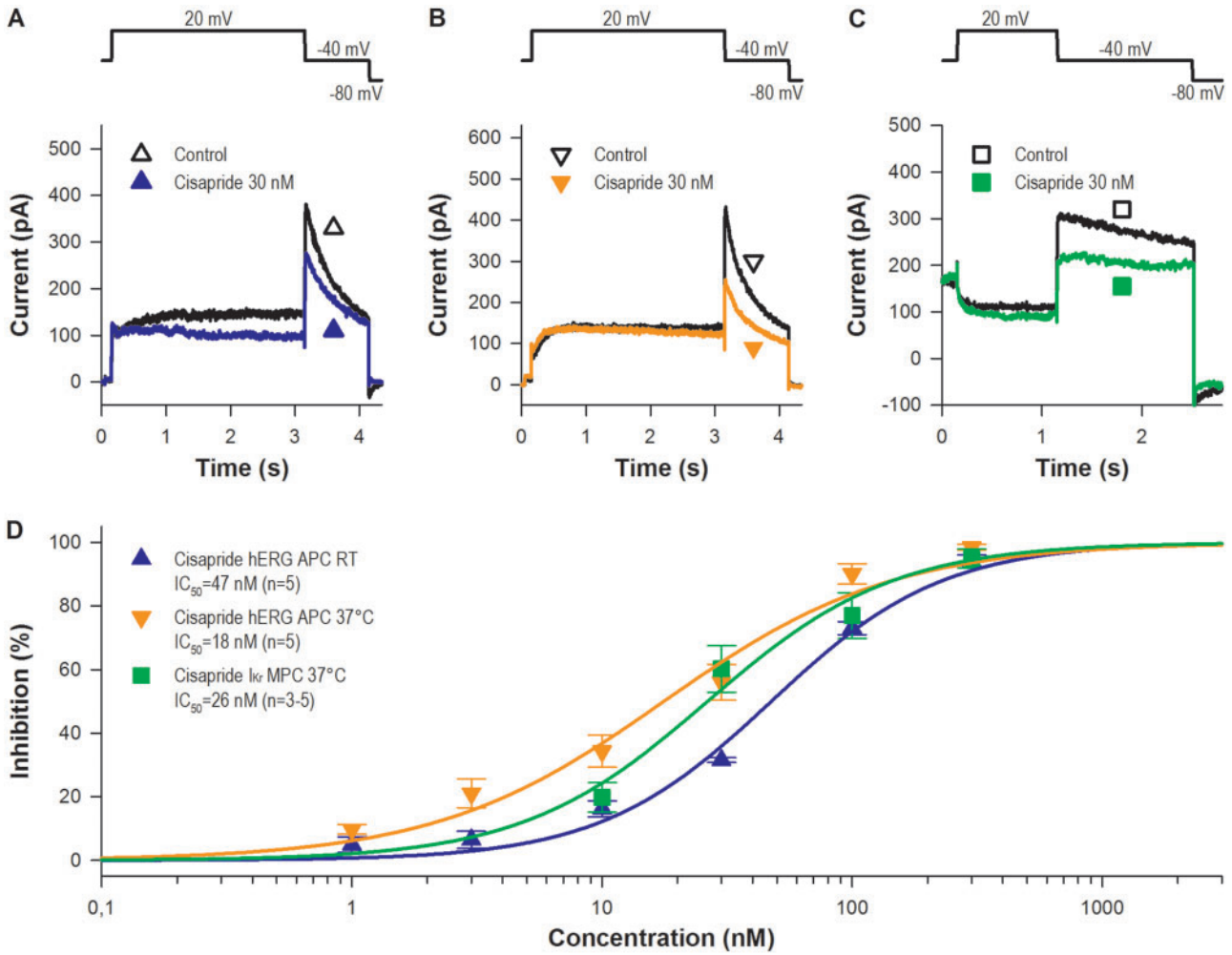

Figure 2. Effect of cisapride on hERG and I_{Kr} current. A, Sample hERG current curves obtained from HEK-hERG cell treated with 30 nM cisapride at room temperature (RT). B, Effect of 30 nM cisapride on hERG current at 37°C. C, Representative I_{Kr} current sweeps obtained from rabbit left ventricular muscle cell treated with 30 nM cisapride. The currents were recorded using the voltage protocols shown at the top of panels (A–C). D, Dose-response curves of cisapride derived from hERG measurements at RT and at 37°C and from I_{Kr} experiments. Abbreviations: APC, automated patch-clamp; MPC, manual patch-clamp.

undiseased human ventricular muscle. As Figure 9 shows, 10 nM dofetilide, 30 nM cisapride, and 30 μM sotalol markedly lengthened the APD at stimulation cycle length of 1000 ms. The prolongation of APD_{90} was 20.4 ± 4.5% ($n = 7$), 27.5 ± 9.8% ($n = 3$), and 28.0 ± 1.8% ($n = 6$), respectively. These values were not significantly different. However, terfenadine even at high 1 μM concentration did not influence the APD at 90% of repolarization (Table 3). Verapamil at 300 nM concentration in 2 experiments did not affect the action potential repolarization in undiseased human right ventricular muscle preparations (Figure 9).

DISCUSSION

Because there are important and not well understood differences between the evaluation of proarrhythmic ability with high-throughput hERG channel, I_{Kr} or action potential experiments, we have studied the effect of 5 drugs with established proarrhythmic potential (dofetilide, cisapride, sotalol, terfenadine, and verapamil) on hERG current (at room temperature and 37°C), on I_{Kr} current (37°C), and on rabbit and human cardiac action potential comparing these assays and helping the rational use of these proarrhythmic pharmacological safety drug tests during preclinical drug development.

Current responses of cells expressing the hERG channel at room temperature and physiological temperature were similar in case of dofetilide. The most noticeable effects of raising the temperature to 37°C were that the peak amplitude was increased, the rise time was decreased and the time constant of decay phase was faster. Despite that, the dose-response curve generated an IC_{50} similar to that obtained at room temperature, and similar to that determined in the I_{Kr} experiments. In addition, these data are in good agreement with our action potential measurements and with previously published data (Mo *et al.*, 2009; Pearlstein *et al.*, 2003; Weerapura *et al.*, 2002).

Conversely, cisapride, sotalol, terfenadine, and verapamil display different potencies at room temperature and 37°C. All these compounds were more potent at physiological temperature and therefore, it is a desirable option to study hERG currents at physiological temperature (Windley *et al.*, 2018). In spite of that, the majority of the commercially available patch-clamp platforms have no integrated temperature control. Apart from the differences in temperature cisapride—like dofetilide—reduced I_{Kr} current and extended the action potential as expected based on hERG measurements, and results are in good agreement with literature (Drolet *et al.*, 1998; Fossa *et al.*, 2004; Martin *et al.*, 2004; Polonchuk, 2012).

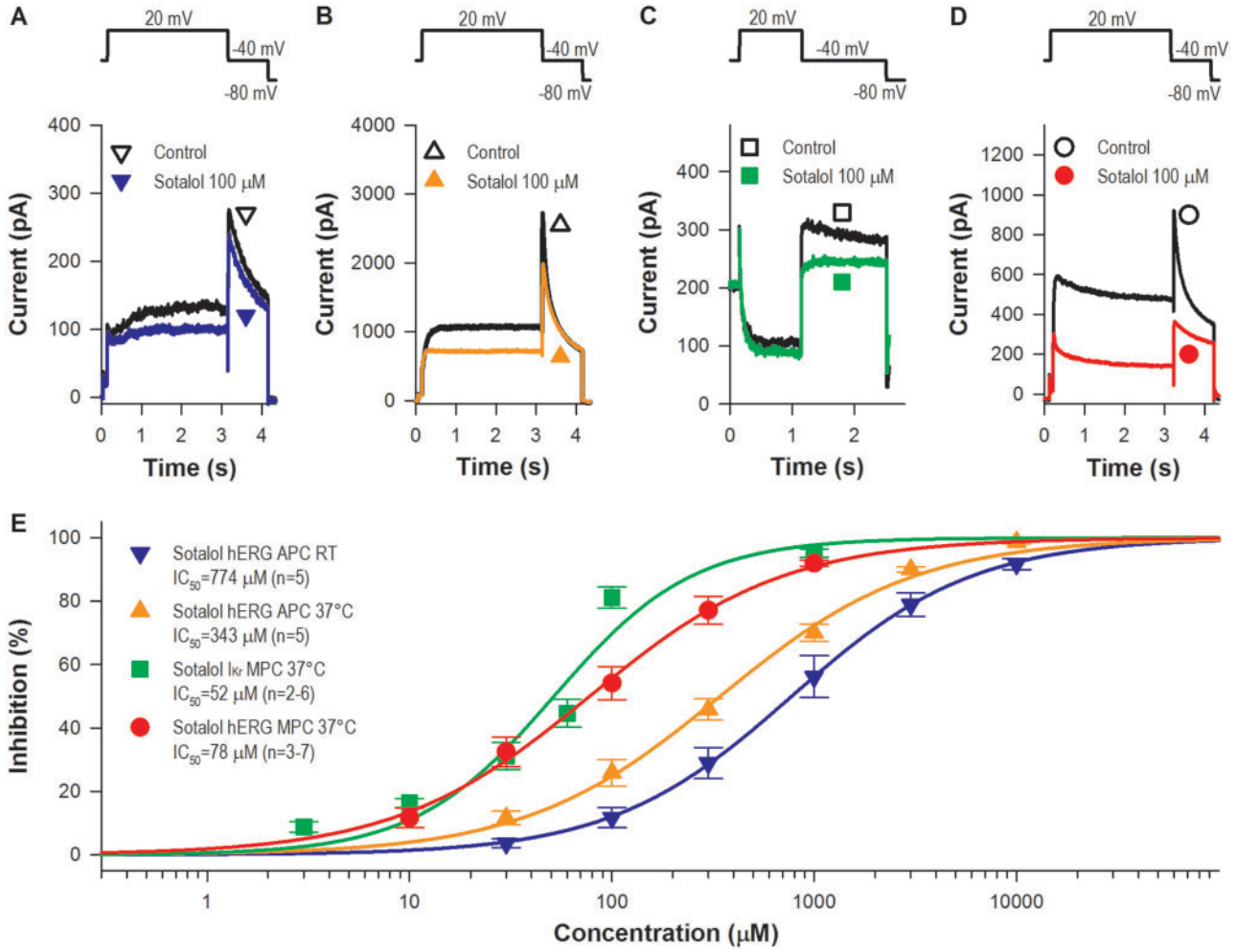

Figure 3. Effect of sotalol on hERG and I_{Kr} current. A, Representative hERG current curves obtained from HEK-hERG cell treated with 100 μM sotalol at room temperature (RT). B, Effect of 100 μM sotalol on hERG current at 37°C. C, Representative I_{Kr} current curves obtained from rabbit left ventricular muscle cell treated with 100 μM sotalol. D, Representative hERG current curves obtained from HEK-hERG cell treated with 100 μM sotalol using manual patch-clamp technique. The currents were recorded using the voltage protocols shown at the top of panels (A–D). E, Concentration-response curves of sotalol obtained from hERG experiments at RT, at 37°C using automated and manual patch-clamp techniques and from I_{Kr} measurements. Abbreviations: APC, automated patch-clamp; MPC, manual patch-clamp.

However, verapamil blocked I_{Kr} current with an IC_{50} value with similar to that calculated from hERG measurements at 37°C but the drug did not lengthen the action potential in rabbit right ventricular preparations. Other studies also reported submicromolar IC_{50} of verapamil for hERG current (Chouabe *et al.*, 1998; Zhang *et al.*, 1999). Zhang *et al.* (1997) described that 1 μM verapamil suppress I_{Kr} tail current by 49% in guinea-pig.

Unlike the other drugs investigated in this study, sotalol and terfenadine showed significantly greater degree of inhibition on I_{Kr} current compared with hERG. In the literature, majority of publications—using mainly manual patch-clamp—reported IC_{50} values for terfenadine between 10 and 60 nM in hERG cell lines, which are much lower than that found in this study. However, higher IC_{50} values have also been reported—for example 950 nM (Abi-Gerges *et al.*, 2011; automated patch-clamp) or 204 nM (Crumb, 2000; manual patch-clamp), and others (Aslanian *et al.*, 2009; Limberis *et al.*, 2006). These later studies used mainly automated patch-clamp method.

In manual patch-clamp, test solutions are usually prepared in relatively large quantities directly before the experiments, and are continuously perfused. In automated platforms, compound plates with minor volume are used, and comparatively small volumes of test solutions are applied to the cells. One may speculate that the adverse surface-to-volume ratio in compound plates and microchannels and the increased incubation time can lead to possible reduction of compound concentrations, especially in case of hydrophobic, "sticky" agents such as terfenadine. Adhesion and precipitation have been identified as the major sources of potential right-shifted less accurate dose-response curves (Mathes, 2006; Mo *et al.*, 2009; Möller and Witchel, 2011), which correspond to the literature data (Carmeliet, 1998; Limberis *et al.*, 2006; Salata *et al.*, 1995). Our experiments showed that the effect of terfenadine on hERG current was stronger measured by the manual patch-clamp technique. The calculated IC_{50} value was similar or even lower (31 vs 54 nM) to that of found in I_{Kr} measurements, which seems to support the assumption explained above. Therefore, the lower efficacy of terfenadine for hERG found in our automated patch-clamp experiments may not reflect the real potency of the drug. In contrast to terfenadine, sotalol is among the least hydrophobic compounds (Mo *et al.*, 2009), and numerous studies also reported extremely high IC_{50} values in hERG cell lines utilized for manual patch-clamp (the half-blocking concentrations of sotalol were 268–1200 μM in these experiments [Abi-Gerges *et al.*, 2011; Guth *et al.*, 2004; Kirsch

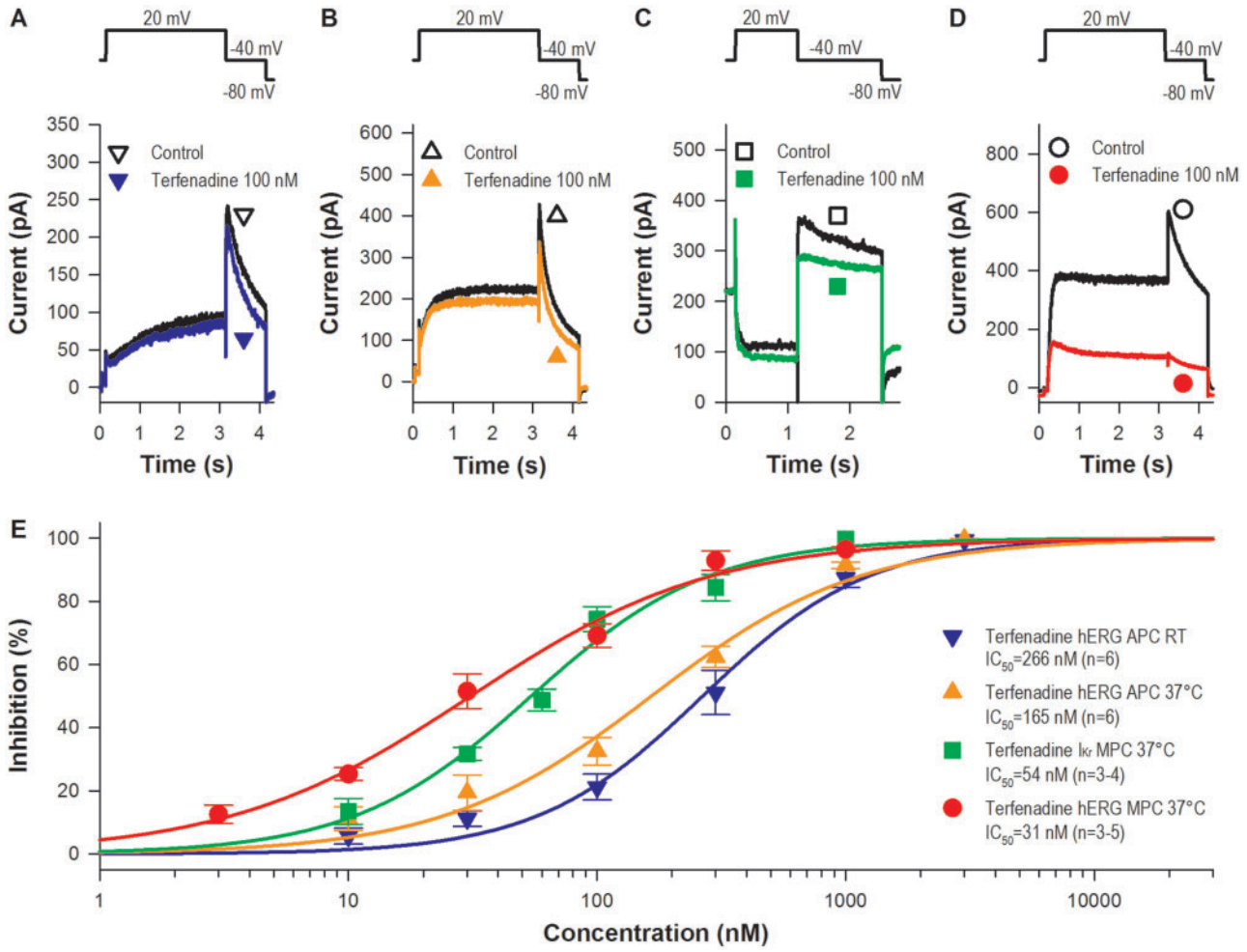

Figure 4. Effect of terfenadine on hERG and I_{Kr} current. A, Representative hERG current sweeps obtained from HEK-hERG cell treated with 100 nM terfenadine at room temperature (RT). B, Effect of 100 nM terfenadine on hERG current at 37°C. C, Representative I_{Kr} current curves obtained from rabbit left ventricular muscle cell treated with 100 nM terfenadine. D, Representative hERG current curves obtained from HEK-hERG cell treated with 100 nM terfenadine using manual patch-clamp technique. The currents were recorded using the voltage protocols shown at the top of panels (A–D). E, Concentration-response curves of terfenadine obtained from hERG experiments at RT, at 37°C using automated and manual patch-clamp techniques and from I_{Kr} measurements. Abbreviations: APC, automated patch-clamp; MPC, manual patch-clamp.

et al., 2004; Perrin et al., 2008; Vormberge et al., 2006]), therefore, this explanation is unlikely. However, IC_{50} value of sotalol calculated from our hERG manual patch-clamp experiments was 77.5 μM showing distinct but moderate difference with the I_{Kr} measurements and it was much less than the corresponding IC_{50} value for automated patch-clamp hERG test. In addition a few study observed similar IC_{50} values for sotalol as such 111 μM (Kramer et al., 2013) and 86 μM (Crumb et al., 2016). Therefore, beyond the high surface-to-volume ratio of recording chips used for automated patch-clamp measurements there should be other important factors, which influence the measurements differently in automated and manual patch-clamp methods.

Also as a possible alternative explanation, the moderate differences between cell line and native myocyte measurements may be due to possible allosteric interaction caused by drugs used in native myocyte but not in cell line measurements for current separation as it was suggested with other organic compound with dofetilide-induced I_{Kr}/hERG inhibition (Yu et al., 2016).

Complex nature of the composition of I_{Kr} channels may also elucidate the difference in potency of sotalol and terfenadine for hERG and native I_{Kr} found in our study. Increasing evidence indicates that the α-subunit composition of the channel can affects its blocking sensitivity. The hERG1 gene encodes at least 2 transcripts: hERG1a, the original isolate, and hERG 1b, an alternate transcript (Lees-Miller et al., 1997; London et al., 1997). The most of hERG screens have been conducted using recombinant cell lines expressing only the hERG 1a subunit, although native ventricular I_{Kr} channels are heteromers containing both hERG 1a and 1b subunits (Jones et al., 2004). Although the potency of most compounds (including sotalol) was similar for the 2 targets, some differences were observed (dofetilide, E-4031 and particularly fluoxetine). Some drugs were more potent at blocking hERG 1a/1b than 1a channels, others exerted greater inhibitory effects on hERG 1a compared with 1a/1b channels. Thus, the existing hERG 1a assays may underestimate the risk of some drugs and overestimate the risk of others (Abi-Gerges et al., 2011; Sale et al., 2008). Also, studies have identified additional interacting proteins affecting hERG drug sensitivity. For example, MinK, MiRPs, and KCR1 coassembles with a pore-forming subunit to create stable complexes whose functional characteristics are similar to the native cardiac potassium

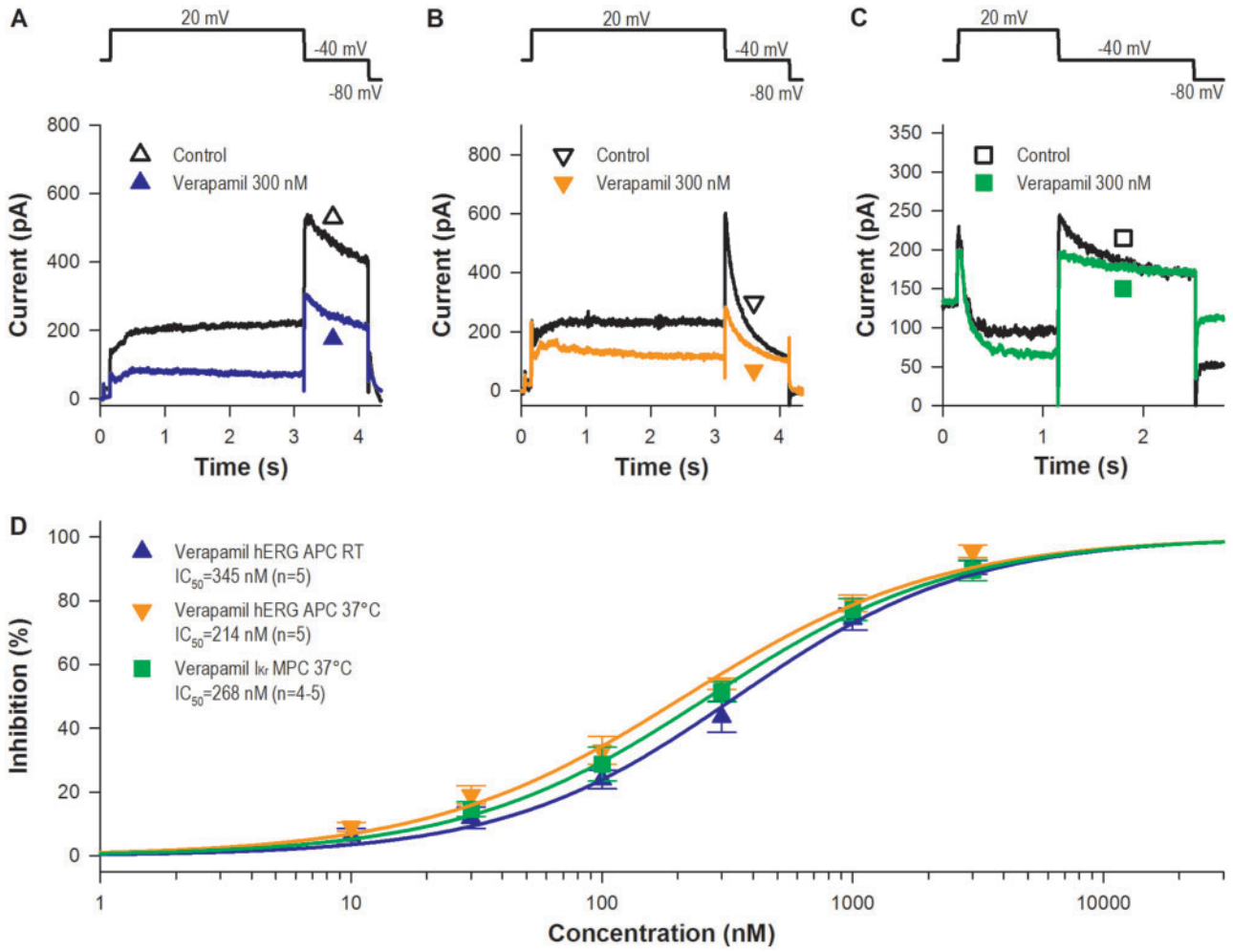

Figure 5. Effect of verapamil on hERG and I_{Kr} current. A, Representative hERG current sweeps obtained from HEK-hERG cell treated with 300 nM verapamil at room temperature (RT). B, Effect of 300 nM verapamil on hERG current at 37°C. C, Representative I_{Kr} current curves obtained from rabbit left ventricular muscle cell treated with 300 nM verapamil. The currents were recorded using the voltage protocols shown at the top of panels (A–C). D, Concentration-response curves of verapamil obtained from hERG experiments at RT and at 37°C using automated patch-clamp technique and from I_{Kr} measurements. Abbreviations: APC, automated patch-clamp; MPC, manual patch-clamp.

Table 1. $IC_{50} \pm$ SEM Values of Inhibitors (Dofetilide, Cisapride, Sotalol, Terfenadine, and Verapamil) Obtained in hERG Assay on Room Temperature (RT), on Physiological (37°C) Temperature and Manual hERG Measurement at 37°C; and in I_{Kr} Assay at 37°C

	Dofetilide (nM)	Cisapride (nM)	Sotalol (μM)	Terfenadine (nM)	Verapamil (nM)
hERG APC RT	8.4 ± 0.2 ($n = 6$)	47.5 ± 4.8 ($n = 5$)	773.7 ± 9.3 ($n = 5$)	266.0 ± 26.8 ($n = 5$)	344.9 ± 26.1 ($n = 5$)
hERG APC 37°C	7.3 ± 0.2 ($n = 5$)	17.7 ± 2.9 ($n = 5$)	342.8 ± 24.8 ($n = 5$)	165.4 ± 24.5 ($n = 5$)	213.6 ± 22.5 ($n = 5$)
hERG MPC 37°C	—	—	77.5 ± 4.8 ($n = 3$–7)	31.0 ± 3.2 ($n = 3$–5)	—
I_{Kr} MPC 37°C	13.0 ± 2.6 ($n = 3$–4)	26.4 ± 4.5 ($n = 3$–5)	51.6 ± 8.8 ($n = 2$–6)	54.3 ± 5.2 ($n = 3$–4)	268.2 ± 11.3 ($n = 4$–5)

Abbreviations: APC, automated patch-clamp; MPC, manual patch-clamp.

channel, adding another level of complexity to mechanisms may affect cardiac safety pharmacology. Their expression and modulation by sotalol could play an important role in determining the amount and character of the I_{Kr} current in individual cardiac myocytes, and may considerably contribute to the action potential prolongation effect of this drug (Abbott *et al.*, 1999; Kupershmidt *et al.*, 2003; McDonald *et al.*, 1997; Weerapura *et al.*, 2002).

Unlike dofetilide, cisapride, and sotalol, terfenadine in spite of inhibiting I_{Kr} had no prolonging effect—even at a high concentration—on APD, which may relate to its blocking effects on other ion channels, such as L-type Ca^{2+} and late Na^{+} currents found in our study, which is the first to report the effect of terfenadine on I_{NaL}. Other studies have also described that terfenadine inhibited not only hERG current but also I_{to}, I_{Ca}, and especially I_{Na} in cardiac myocytes (Ducic *et al.*, 1997; Hondeghem *et al.*, 2011; Lu and Wang, 1999).

Similarly to terfenadine, verapamil did not lengthen the action potential duration. It is known for a long time that verapamil is a Ca-antagonist and as such it blocks L-type Ca^{2+} current (Ehara and Daufmann, 1978; Kohlhardt *et al.*, 1972). Zhang *et al.* (1997) found that application of verapamil at 1 and 5 μM induced

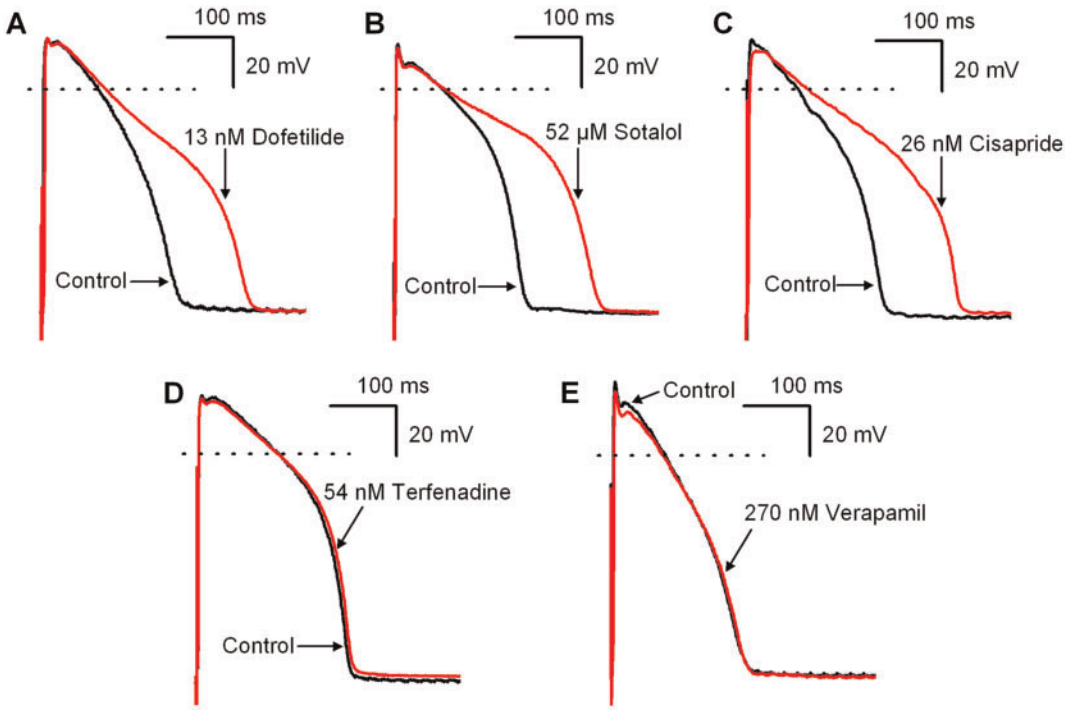

Figure 6. The effects of 13 nM dofetilide (A), 52 μM sotalol (B), 26 nM cisapride (C), 54 nM terfenadine (D), and 270 nM verapamil (E) on action potential waveform of rabbit ventricular muscle at basic cycle length of 1000 ms.

Table 2. The Electrophysiological Effects of 13 nM Dofetilide ($n = 7$), 26 nM Cisapride ($n = 6$), 52 μM Sotalol ($n = 5$), 54 nM Terfenadine ($n = 8$), and 270 nM Verapamil ($n = 5$) in Rabbit Ventricular Muscle Preparations at Basic Cycle Length of 1000 ms

	RP (mV)	APA (mV)	V_{max} (V/s)	APD_{90} (ms)	APD_{90} (%)	APD_{50} (ms)
Control	−88.3 ± 0.3	109.0 ± 2.4	182.1 ± 12.4	190.5 ± 14.1		154.7 ± 15.1
Dofetilide 13 nM	−87.6 ± 0.8	109.3 ± 3.5	187.0 ± 15.9	285.9 ± 40.1*	47.8 ± 12.9	234.4 ± 38.2*
Control	−89.7 ± 0.6	105.1 ± 2.0	139.7 ± 14.0	184.7 ± 6.9		143.0 ± 7.7
Cisapride 26 nM	−88.7 ± 1.3	105.7 ± 1.7	129.3 ± 14.8	310.7 ± 20.7*	68.4 ± 10.0	236.3 ± 18.3*
Control	−90.1 ± 0.7	103.4 ± 1.9	170.5 ± 15.3	156.9 ± 10.7		116.6 ± 13.1
Sotalol 52 μM	−91.8 ± 0.6	105.8 ± 3.1	205.3 ± 21.6	244.3 ± 15.9*	56.0 ± 4.6	181.3 ± 21.5*
Control	−91.5 ± 0.6	111.9 ± 1.9	179.9 ± 10.5	205.4 ± 9.1		170.1 ± 9.0
Terfenadine 54 nM	−91.1 ± 1.2	113.7 ± 2.3	201.5 ± 18.5	209.1 ± 13.7	1.4 ± 3.0	174.5 ± 13.0
Control	−84.1 ± 2.2	104.7 ± 2.9	129.3 ± 13.8	176.6 ± 11.5		139.5 ± 13.1
Verapamil 270 nM	−81.6 ± 2.2	105.8 ± 1.9	121.9 ± 12.1	177.3 ± 12.6	0.6 ± 1.8	137.2 ± 14.0

Results are means ± SEM. *$p < .05$.

Abbreviations: APA, action potential amplitude; APD_{90} and APD_{50}, action potential durations at 50% and 90% of repolarization; RP, resting potential; V_{max}, maximum rate of depolarization.

dual changes in repolarization, prolonging APD_{90} at 1 μM, and shortening at 5 μM in guinea-pig isolated myocytes, however, Chen and Gettes (1979) reported that verapamil did not influence APD in guinea-pig and dog papillary muscles. In our study, the I_{CaL} blocking property of verapamil found to be similar or even weaker than the I_{Kr} blocking potency of the drug. I_{NaL} was not affected by verapamil in our experiments, similarly to earlier studies reporting that verapamil at similar concentration range did not influence fast Na^+ current (Chen and Gettes, 1979; Rosen *et al.*, 1975).

Therefore, the multichannel blocking property of terfenadine and verapamil might explain the lack of action potential prolonging effect of these drugs. It is interesting that dofetilide, cisapride, and sotalol produced a more excessive lengthening of APD in rabbit ventricular tissue preparations compared with that found in human. Thus, there may be species differences in the effects of I_{Kr} blockade, which emphasizes the importance of species model selected for a safety pharmacological study. The expression level and properties of cardiac ion channels are varied in different species that should be taken into account when extrapolating the results from animal models of proarrhythmia to humans. Some studies (Jonsson *et al.*, 2012; Liang *et al.*, 2013; Scheel *et al.*, 2014) using a relatively new approach, the human stem cell-derived cardiomyocytes, and recently 2 other papers (Page *et al.*, 2016; Qu *et al.*, 2018) that applied the conventional microelectrode technique in human ventricular trabeculae investigated possible pro-arrhythmia risk of several drugs including dofetilide, cisapride, terfenadine, sotalol, and verapamil. Our action potential data obtained from human preparations are in good agreement with the results of Qu *et al.* (2018) except

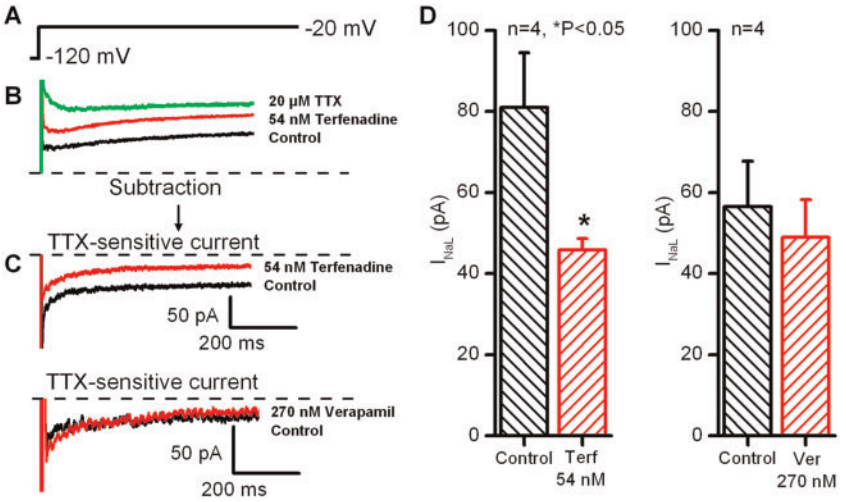

Figure 7. Effect of 54 nM terfenadine and 270 nM verapamil on I_{NaL} current in rabbit ventricular myocytes. A, Applied voltage protocol. B, Original current traces show that 54 nM terfenadine excessively reduced I_{NaL}, whereas 20 μM TTX completely blocks the current. C, TTX sensitive current traces in control conditions and after application of 54 nM terfenadine (*top*) and 270 nM verapamil (*bottom*). D, TTX sensitive current (I_{NaL}) in the absence and presence of 54 nM terfenadine (*left*) and 270 nM verapamil (*right*) at the test potential of −20 mV. Values are means ± SEM, $n = 4$, $^*p < .05$.

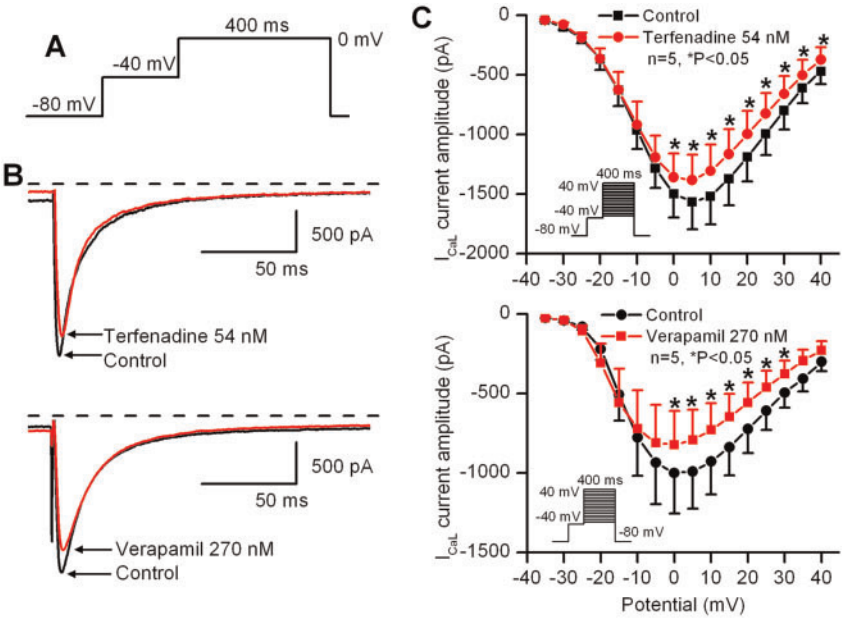

Figure 8. Effect of 54 nM terfenadine and 270 nM verapamil on the L-type I_{Ca} in rabbit ventricular myocytes. A, Voltage protocol. B, Original current traces recorded in control conditions and in the presence of 54 nM terfenadine (*top*) and 270 nM verapamil (*bottom*). C, Current-voltage relationship of I_{CaL} in the absence and presence of 54 nM terfenadine (*top*) and 270 nM verapamil (*bottom*). Values are means ± SEM, $n = 5$, $^*p < .05$.

for cisapride. Qu *et al.* (2018) reported that 30 nM cisapride slightly (by 8%) shortened the action potential. Page *et al.* (2016), however, described similar results with dofetilide, sotalol, and verapamil to that found in this study. Therefore, human *ex vivo* models using native human ventricular preparations would generate more reliable and predictive data on proarrhythmic adverse effects at the preclinical stage of drug development (Page *et al.*, 2016).

As the hERG assay is pulse protocol sensitive, longer pulses and higher frequency would potentiate the drug binding to the channel increasing the potency of the drug depending on the onset and offset kinetics of the compound (Kirsch *et al.*, 2004). Therefore, a shorter impulse, such as an action potential, which is only about 200 ms long in rabbit heart, might decrease the chance of drug binding influencing negatively the potency of a particular drug during action potential measurements.

Another factor might affect the potency of a drug is that during these experiments the drug must penetrate into the tissue preparation to exert its effects. Slow diffusion of drug in the tissue may result in low tissue concentration, which impairs the effect of a particular drug on action potential repolarization.

These additional factors may offset repolarization lengthening of terfenadine and verapamil. I_{Na} blockade of the terfenadine can impair impulse conduction, thus evoke ventricular fibrillation, related to a noticeable widening of the QRS complex, without significant prolongation of QT intervals (Hondeghem *et al.*, 2011; Lu *et al.*, 2012). In this context it has to mention that in this manuscript we did not focus on the accuracy of

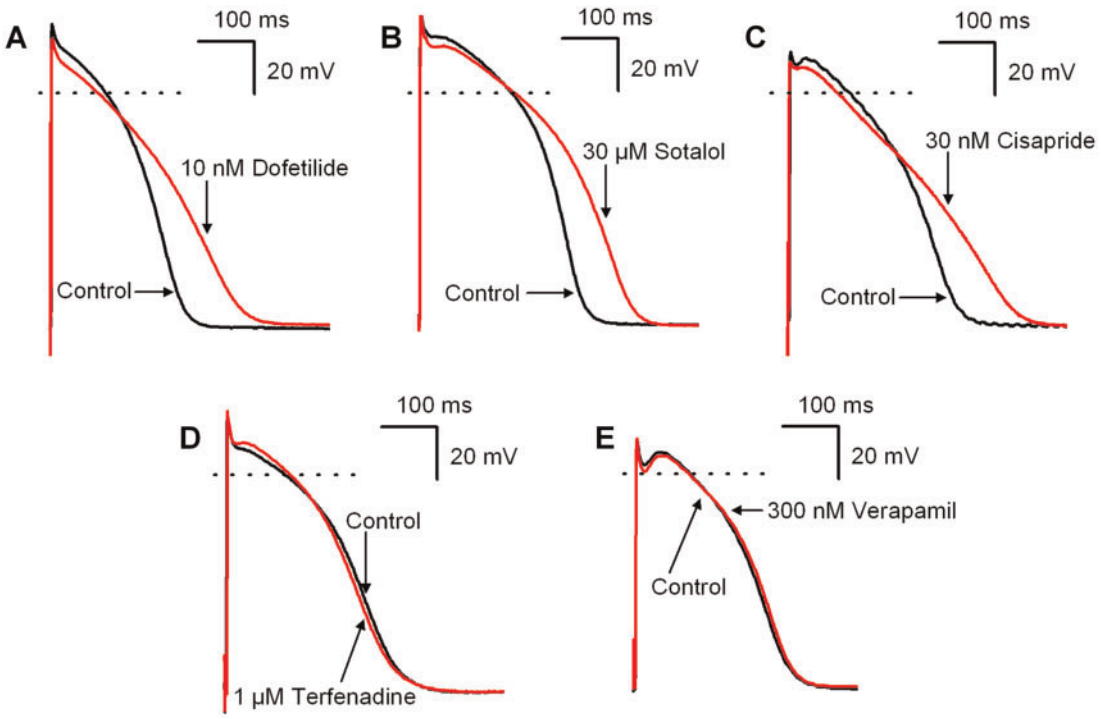

Figure 9. The effects of 10 nM dofetilide (A), 30 μM sotalol (B), 30 nM cisapride (C), 1 μM terfenadine (D), and 300 nM verapamil (E) on action potential waveform in undiseased human ventricular muscle at basic cycle length of 1000 ms.

Table 3. The Electrophysiological Effects of 10 nM Dofetilide ($n = 7$), 30 nM Cisapride ($n = 3$), 30 μM Sotalol ($n = 6$), 1 μM Terfenadine ($n = 3$), and 300 nM Verapamil ($n = 3$) in Human Ventricular Muscle Preparations at Basic Cycle Length of 1000 ms

	RP (mV)	APA (mV)	V_{max} (V/s)	APD_{90} (ms)	APD_{90} (%)	APD_{50} (ms)
Control	−86.9 ± 1.3	110.1 ± 1.4	295.5 ± 35.7	239.4 ± 9.8		180.0 ± 6.7
Dofetilide 10 nM	−87.4 ± 0.8	110.9 ± 2.6	263.4 ± 28.9	287.6 ± 13.6*	20.4 ± 4.5	206.6 ± 7.9*
Control	−83.7 ± 5.0	103.3 ± 2.5	265.9 ± 71.0	260.7 ± 17.8		180.4 ± 19.8
Cisapride 30 nM	−83.9 ± 3.5	102.3 ± 1.8	269.8 ± 61.8	334.6 ± 42.1	27.5 ± 9.8	224.6 ± 22.2
Control	−89.7 ± 1.0	119.2 ± 2.0	230.8 ± 21.3	301.8 ± 19.7		233.0 ± 17.4
Sotalol 30 μM	−88.8 ± 1.5	119.2 ± 2.4	250.0 ± 21.1	387.0 ± 27.6*	28.0 ± 1.8	281.0 ± 20.1*
Control	−84.8 ± 1.9	109.7 ± 3.2	275.9 ± 26.6	269.7 ± 12.7		208.7 ± 10.3
Terfenadine 1 μM	−84.6 ± 1.7	112.4 ± 3.0	325.2 ± 34.6	256.7 ± 16.6	−5.0 ± 1.7	192.0 ± 9.4*
Control	−87.8 ± 2.8	99.1 ± 7.8	203.2 ± 63.3	262.1 ± 17.2		194.4 ± 16.5
Verapamil 300 nM	−90.7 ± 0.8	101.5 ± 6.3	213.3 ± 61.1	270.7 ± 11.2	3.6 ± 2.7	199.9 ± 12.4

Results are means ± SEM. *$p < .05$.

Abbreviations: APA, action potential amplitude; APD_{90} and APD_{50}, action potential durations at 50% and 90% of repolarization; RP, resting potential; V_{max}, maximum rate of depolarization.

predictability of drug-induced TdP or ventricular fibrillation. Other recent well-demonstrated studies strongly suggest that other factors than potassium ion channel inhibition such as Triangulation of action potential waveform, Reverse use dependence, Instability, and Dispersion of repolarization defined as TRIaD and wavelength of excitation (λ) defined as CV (conduction velocity) multiplied by the effective refractory period (ERP) are also important to properly assess drug-induced arrhythmia propensity (Hondeghem, 2008a,b). In our work, we only would like to present further arguments regarding the shortcomings of the widely used hERG screening for arrhythmia predictability.

According to our research, native I_{Kr} assay shows better correlation with APD than hERG measurements and it seems a better tool in evaluation of cardiac proarrhythmic risk. Although it is generally accepted that the most common electrophysiological mechanism for drug-associated cardiac proarrhythmic and sudden death risks result from blocking I_{Kr}, accordingly, inhibition of I_{Kr} current is considered a primary detector for proarrhythmic liability, the possibility of inhibition of other potassium currents such as I_{K1} and I_{Ks} cannot be neglected. It was shown that malfunction of those latter ion channels can cause latent and manifest LQT syndromes (Cubeddu, 2016). Also blocking these K^+ channels may not result in marked repolarization lengthening but by decreasing the repolarization reserve they greatly increase dispersion of repolarization and thereby enhancing proarrhythmic risk (Biliczki *et al.*, 2002; Roden, 2008; Roden and Yang, 2005). Therefore, careful safety pharmacological testing should also include preparation where the repolarization reserve had been previously attenuated to reveal this apparently silent proarrhythmic risk. It

should be kept in mind that drug-induced proarrhythmic events may have very low incidence (1:10 000–1:100 000) suggesting that multiple channel hits can be 1 possible explanation (Hancox *et al.*, 2008; Lengyel *et al.*, 2007; Varró and Baczkó, 2011; Yap and Camm, 2003). However, drugs, such as amiodarone or ranolazine can induce large action potential lengthening and QT prolongation with a concomitant reduction of the dispersion of repolarization in the ventricle decreasing the risk of arrhythmia. It is most likely due to the multichannel (I_{Kr}, I_{Ks}, I_{Na}, and I_{CaL}) blockade of these drugs especially inhibition of the late I_{Na}, which current is more prominent in the midmyocardial cells and in Purkinje fibers (Antzelevitch *et al.*, 2004). In other words, complex multichannel interactions of drugs with other cardiac ion channels can also contribute to their proarrhythmic effects—but also sometimes tend to mitigate the proarrhythmic effect of I_{Kr} current blockade—thus action potential and *in vivo* cardiac electrophysiological measurements also should be an integral part of proarrhythmic pharmacological safety drug tests, the single ion channel approach is not recommended. Moreover, *in vitro* and *in vivo* studies with reduced repolarization reserve are also essential, adding another level to the cardiac safety pharmacology.

In conclusion, results obtained with automated patch-clamp equipment in HEK-hERG cells usually show a reasonable conformity with outcomes of I_{Kr} current and action potential experiments. However, important and not well understood differences exist between the evaluation of hERG-blocking ability with automated patch-clamp and other techniques such as the I_{Kr}, action potential, and ECG measurements. Therefore, cardiac safety is more accurately evaluated using all these methods simultaneously. The application of high-throughput hERG channel screening as the only or predominant method is not recommended because it may discredit otherwise valuable lead molecules and/or may not detect properly the proarrhythmic potentials of others. This study would like to draw the attention to the limitations of the single ion channel approach especially using high-throughput screening. In recent years, great efforts have been made on improving the assessment of drug-associated TdP risk. The purpose of the comprehensive *in vitro* proarrhythmia assay is to avoid the misidentification of proarrhythmic potential of drugs based only on hERG and QT investigations (Sager *et al.*, 2014). This new paradigm consist of 4 components: an ion channel panel measured in heterologous expression systems, *in silico* action potential models, human-induced pluripotent stem cell-derived cardiomyocyte assay, and human phase 1 ECGs. Based on our studies, characterization of electrophysiological effects of drugs and drug candidate molecules on native ion channels and animal or especially human *ex-vivo* action potential models are also important, and may contribute to the understanding of the complex proarrhythmic mechanisms. However, additional studies with much larger set of compounds are needed to infer the true predictivity of the integrated hERG, I_{Kr}, and AP/ECG assays.

Limitation of the Study

Important transmural and regional differences in current densities and in ion channel subunit protein expression exist within the heart. However, in our study ion currents were measured in single myocytes (mainly midmyocardial) isolated from left ventricular tissue, but action potentials were recorded from right ventricular subendocardial tissue. The reason is mainly technical. Conventional microelectrode recordings from left ventricular tissue were difficult to obtain producing a substantially smaller success rate and left ventricular subendocardial tissue more likely to be contaminated by subendocardial Purkinje cells, which electrotonically influence the recordings and hamper pharmacologic investigations.

Another issue is the problem of species differences. Most of our experiments were performed in rabbit. However, the action potential waveform in rabbit is similar to that of human but the current density, kinetical properties and even the type of channel subunits in rabbit may be different from those in human, which may influence the drug effects on action potential and repolarization.

The third factor is that experimental conditions such as voltage protocol, stimulation frequency, exposure time of the drug, and temperature may affect the action of drugs. If the particular drug rate- or voltage-dependently block the channel its potency in patch-clamp experiments may diverged from that measured in physiological conditions in cardiac muscle.

ACKNOWLEDGMENTS

The authors wish to thank Mrs Zsuzsa Molnár for technical assistance. The authors have declared that no conflicts of interest exist.

FUNDING

This work was supported by grants from the National Research, Development and Innovation Office (K-119992, FK-129117, and a GINOP-2.3.2-15-2016-00012), the Ministry of Human Capacities Hungary (20391-3/2018/FEKUSTRAT and EFOP-3.6.2-16-2017-00006), by the HU-RO Cross-Border Cooperation Programmes (HU-RO/0802/011_AF HURO-CARDIOPOL and HURO/1001/086/2.2.1 HURO-TWIN) and from the Hungarian Academy of Sciences.

REFERENCES

Abbott, G. W., Sesti, F., Splawski, I., Buck, M. E., Lehmann, M. H., Timothy, K. W., Keating, M. T., and Goldstein, S. A. (1999). MiRP1 forms I_{Kr} potassium channels with hERG and is associated with cardiac arrhythmia. *Cell* **97**, 175–187.

Abi-Gerges, N., Holkham, H., Jones, E. M. C., Pollard, C. E., Valentin, J.-P., and Robertson, G. A. (2011). hERG subunit composition determines differential drug sensitivity. *Br. J. Pharmacol.* **164**, 419–432.

Alexander, S. P. H., Mathie, A., and Peters, J. A. (2011). Guide to Receptors and Channels (GRAC), 5th edition. *Br. J. Pharmacol.* **164(Suppl. 1)**, S1–324.

Antzelevitch, C., Belardinelli, L., Zygmunt, A. C., Burashnikov, A., Di Diego, J. M., Fish, J. M., Cordeiro, J. M., and Thomas, G. (2004). Electrophysiological effects of ranolazine, a novel antianginal agent with antiarrhythmic properties. *Circulation* **110**, 904–910.

Aslanian, R., Piwinski, J. J., Zhu, X., Priestley, T., Sorota, S., Du, X. Y., Zhang, X. S., McLeod, R. L., West, R. E., and Williams, S. M. (2009). Structural determinants for histamine H(1) affinity, hERG affinity and QTc prolongation in a series of terfenadine analogs. *Bioorg. Med. Chem. Lett.* **19**, 5043–5047.

Biliczki, P., Virág, L., Iost, N., Papp, J. G., and Varró, A. (2002). Interaction of different potassium channels in cardiac repolarization in dog ventricular preparations: Role of repolarization reserve. *Br. J. Pharmacol.* **137**, 361–368.

Carmeliet, E. (1998). Effects of cetirizine on the delayed K^+ currents in cardiac cells: Comparison with terfenadine. *Br. J. Pharmacol.* **124**, 663–668.

Chen, C. M., and Gettes, L. S. (1979). Effects of verapamil on rapid Na channel-dependent action potentials of K^+-depolarized ventricular fibers. *J. Pharmacol. Exp. Ther.* **209**, 415–421.

Chouabe, C., Drici, M. D., Romey, G., Barhanin, J., and Lazdunski, M. (1998). hERG and KvLQT1/IsK, the cardiac K^+ channels involved in long QT syndromes, are targets for calcium channel blockers. *Mol. Pharmacol.* **54**, 695–703.

Crumb, W. J., Jr (2000). Loratadine blockade of K(+) channels in human heart: Comparison with terfenadine under physiological conditions. *J. Pharmacol. Exp. Ther.* **292**, 261–264.

Crumb, W. J., Jr, Vicente, J., Johannesen, L., and Strauss, D. G. (2016). An evaluation of 30 clinical drugs against the comprehensive *in vitro* proarrhythmia assay (CiPA) proposed ion channel panel. *J. Pharmacol. Toxicol. Methods* **81**, 251–262.

Cubeddu, L. X. (2016). Drug-induced inhibition and trafficking disruption of ion channels: Pathogenesis of QT abnormalities and drug-induced fatal arrhythmias. *Curr. Cardiol. Rev.* **12**, 141–154.

Dabrowski, M. A., Dekermendjian, K., Lund, P.-E., Krupp, J. J., Sinclair, J., and Larsson, O. (2008). Ion channel screening technology. *CNS Neurol. Disord. Drug Targets* **7**, 122–128.

Drolet, B., Khalifa, M., Daleau, P., Hamelin, B. A., and Turgeon, J. (1998). Block of the rapid component of the delayed rectifier potassium current by the prokinetic agent cisapride underlies drug-related lengthening of the QT interval. *Circulation* **97**, 204–210.

Ducic, I., Ko, C. M., Shuba, Y., and Morad, M. (1997). Comparative effects of loratadine and terfenadine on cardiac K^+ channels. *J. Cardiovasc. Pharmacol.* **30**, 42–54.

Dunlop, J., Bowlby, M., Peri, R., Vasilyev, D., and Arias, R. (2008). High-throughput electrophysiology: An emerging paradigm for ion-channel screening and physiology. *Nat. Rev. Drug Discov.* **7**, 358–368.

Ehara, T., and Daufmann, R. (1978). The voltage- and time-dependent effects of (−)-verapamil on the slow inward current in isolated cat ventricular myocardium. *J. Pharmacol. Exp. Ther.* **207**, 49–55.

Farre, C., and Fertig, N. (2012). HTS techniques for patch clamp-based ion channel screening—advances and economy. *Expert Opin. Drug Discov.* **7**, 515–524.

Farre, C., George, M., Brüggemann, A., and Fertig, N. (2008). Ion channel screening—automated patch clamp on the rise. *Drug Discov. Today Technol.* **5**, e23–28.

Farre, C., Haythornthwaite, A., Haarmann, C., Stoelzle, S., Kreir, M., George, M., Brüggemann, A., and Fertig, N. (2009). Port-a-patch and patchliner: High fidelity electrophysiology for secondary screening and safety pharmacology. *Comb. Chem. High Throughput Screen.* **12**, 24–37.

Farre, C., Stoelzle, S., Haarmann, C., George, M., Brüggemann, A., and Fertig, N. (2007). Automated ion channel screening: Patch clamping made easy. *Expert Opin. Ther. Targets* **11**, 557–565.

Fertig, N., Blick, R. H., and Behrends, J. C. (2002). Whole cell patch clamp recording performed on a planar glass chip. *Biophys. J.* **82**, 3056–3062.

Fossa, A. A., Wisialowski, T., Wolfgang, E., Wang, E., Avery, M., Raunig, D. L., and Fermini, B. (2004). Differential effect of hERG blocking agents on cardiac electrical alternans in the guinea pig. *Eur. J. Pharmacol.* **486**, 209–221.

Guth, B. D., Germeyer, S., Kolb, W., and Markert, M. (2004). Developing a strategy for the nonclinical assessment of proarrhythmic risk of pharmaceuticals due to prolonged ventricular repolarization. *J. Pharmacol. Toxicol. Methods* **49**, 159–169.

Hancox, J. C., McPate, M. J., El Harchi, A., and Zhang, Y. H. (2008). The hERG potassium channel and hERG screening for drug-induced torsades de pointes. *Pharmacol. Ther.* **119**, 118–132.

Hishigaki, H., and Kuhara, S. (2011). hERGAPDbase: A database documenting hERG channel inhibitory potentials and APD-prolongation activities of chemical compounds. *Database J. Biol. Databases Curation* **2011**, bar017.

Hodgkin, A. L., and Huxley, A. F. (1945). Resting and action potentials in single nerve fibres. *J. Physiol.* **104**, 176–195.

Hondeghem, L. M. (2008a). QT prolongation is an unreliable predictor of ventricular arrhythmia. *Heart Rhythm* **5**, 1210–1212.

Hondeghem, L. M. (2008b). Use and abuse of QT and TRIaD in cardiac safety research: Importance of study design and conduct. *Eur. J. Pharmacol.* **584**, 1–9.

Hondeghem, L. M., Dujardin, K., Hoffmann, P., Dumotier, B., and De Clerck, F. (2011). Drug-induced QT_C prolongation dangerously underestimates proarrhythmic potential: Lessons from terfenadine. *J. Cardiovasc. Pharmacol.* **57**, 589–597.

Jones, E. M. C., Roti Roti, E. C., Wang, J., Delfosse, S. A., and Robertson, G. A. (2004). Cardiac I_{Kr} channels minimally comprise hERG 1a and 1b subunits. *J. Biol. Chem.* **279**, 44690–44694.

Jonsson, M. K., Vos, M. A., Mirams, G. R., Duker, G., Sartipy, P., de Boer, T. P., and van Veen, T. A. (2012). Application of human stem cell-derived cardiomyocytes in safety pharmacology requires caution beyond hERG. *J. Mol. Cell. Cardiol.* **52**, 998–1008.

Jost, N., Nagy, N., Corici, C., Kohajda, Z., Horváth, A., Acsai, K., Biliczki, P., Levijoki, J., Pollesello, P., Koskelainen, T., *et al.* (2013). ORM-10103, a novel specific inhibitor of the $Na^+/Ca2^+$ exchanger, decreases early and delayed afterdepolarizations in the canine heart. *Br. J. Pharmacol.* **170**, 768–778.

Jost, N., Virág, L., Bitay, M., Takács, J., Lengyel, C., Biliczki, P., Nagy, Z., Bogáts, G., Lathrop, D. A., Papp, J. G., *et al.* (2005). Restricting excessive cardiac action potential and QT prolongation: A vital role for I_{Ks} in human ventricular muscle. *Circulation* **112**, 1392–1399.

Kirsch, G. E., Trepakova, E. S., Brimecombe, J. C., Sidach, S. S., Erickson, H. D., Kochan, M. C., Shyjka, L. M., Lacerda, A. E., and Brown, A. M. (2004). Variability in the measurement of hERG potassium channel inhibition: Effects of temperature and stimulus pattern. *J. Pharmacol. Toxicol. Methods* **50**, 93–101.

Kohajda, Z., Farkas-Morvay, N., Jost, N., Nagy, N., Geramipour, A., Horváth, A., Varga, R. S., Hornyik, T., Corici, C., Acsai, K., *et al.* (2016). The effect of a novel highly selective inhibitor of the sodium/calcium exchanger (NCX) on cardiac arrhythmias in *in vitro* and *in vivo* experiments. *PLoS One* **11**, e0166041.

Kohlhardt, M., Bauer, B., Krause, H., and Fleckenstein, A. (1972). Na and Ca channels in mammalian cardiac fibres by the use of specific inhibitors. *Pflugers Arch.* **335**, 309–322.

Kramer, J., Obejero-Paz, C. A., Myatt, G., Kuryshev, Y. A., Bruening-Wright, A., Verducci, J. S., and Brown, A. M. (2013). MICE models: Superior to the hERG model in predicting torsade de pointes. *Sci. Rep.* **3**, 2100.

Kristóf, A., Husti, Z., Koncz, I., Kohajda, Z., Szél, T., Juhász, V., Biliczki, P., Jost, N., Baczkó, I., Papp, J. G., *et al.* (2012). Diclofenac prolongs repolarization in ventricular muscle with impaired repolarization reserve. *PLoS One* **7**, e53255.

Kupershmidt, S., Yang, I. C.-H., Hayashi, K., Wei, J., Chanthaphaychith, S., Petersen, C. I., Johns, D. C., George, A. L., Roden, D. M., and Balser, J. R. (2003). The I_{Kr} drug response is modulated by KCR1 in transfected cardiac and noncardiac cell lines. *FASEB J.* **17**, 2263–2265.

Lees-Miller, J. P., Kondo, C., Wang, L., and Duff, H. J. (1997). Electrophysiological characterization of an alternatively processed ERG K^+ channel in mouse and human hearts. *Circ. Res.* **81**, 719–726.

Lengyel, C., Iost, N., Virág, L., Varró, A., Lathrop, D. A., and Papp, J. G. (2001). Pharmacological block of the slow component of the outward delayed rectifier current (*I*(Ks)) fails to lengthen rabbit ventricular muscle QT(c) and action potential duration. *Br. J. Pharmacol.* **132**, 101–110.

Lengyel, C., Varró, A., Tábori, K., Papp, J. G., and Baczkó, I. (2007). Combined pharmacological block of *I*(Kr) and *I*(Ks) increases short-term QT interval variability and provokes torsades de pointes. *Br. J. Pharmacol.* **151**, 941–951.

Liang, P., Lan, F., Lee, A. S., Gong, T., Sanchez-Freire, V., Wang, Y., Diecke, S., Sallam, K., Knowles, J. W., Wang, P. J., *et al.* (2013). Drug screening using a library of human induced pluripotent stem cell-derived cardiomyocytes reveals disease-specific patterns of cardiotoxicity. *Circulation* **127**, 1677–1691.

Limberis, J. T., Su, Z., Cox, B. F., Gintant, G. A., and Martin, R. L. (2006). Altering extracellular potassium concentration does not modulate drug block of human ether-a-go-go-related gene (hERG) channels. *Clin. Exp. Pharmacol. Physiol.* **33**, 1059–1065.

London, B., Trudeau, M. C., Newton, K. P., Beyer, A. K., Copeland, N. G., Gilbert, D. J., Jenkins, N. A., Satler, C. A., and Robertson, G. A. (1997). Two isoforms of the mouse ether-a-go-go-related gene coassemble to form channels with properties similar to the rapidly activating component of the cardiac delayed rectifier K^+ current. *Circ. Res.* **81**, 870–878.

Lü, Q., and An, W. F. (2008). Impact of novel screening technologies on ion channel drug discovery. *Comb. Chem. High Throughput Screen.* **11**, 185–194.

Lu, H. R., Hermans, A. N., and Gallacher, D. J. (2012). Does terfenadine-induced ventricular tachycardia/fibrillation directly relate to its QT prolongation and torsades de pointes? *Br. J. Pharmacol.* **166**, 1490–1502.

Lu, Y., and Wang, Z. (1999). Terfenadine block of sodium current in canine atrial myocytes. *J. Cardiovasc. Pharmacol.* **33**, 507–513.

Martin, R. L., McDermott, J. S., Salmen, H. J., Palmatier, J., Cox, B. F., and Gintant, G. A. (2004). The utility of hERG and repolarization assays in evaluating delayed cardiac repolarization: Influence of multi-channel block. *J. Cardiovasc. Pharmacol.* **43**, 369–379.

Mathes, C. (2006). QPatch: The past, present and future of automated patch clamp. *Expert Opin. Ther. Targets* **10**, 319–327.

McDonald, T. V., Yu, Z., Ming, Z., Palma, E., Meyers, M. B., Wang, K. W., Goldstein, S. A., and Fishman, G. I. (1997). A minK-hERG complex regulates the cardiac potassium current *I*(Kr). *Nature* **388**, 289–292.

Mo, Z.-L., Faxel, T., Yang, Y.-S., Gallavan, R., Messing, D., and Bahinski, A. (2009). Effect of compound plate composition on measurement of hERG current IC(50) using PatchXpress. *J. Pharmacol. Toxicol. Methods* **60**, 39–44.

Möller, C., and Witchel, H. (2011). Automated electrophysiology makes the pace for cardiac ion channel safety screening. *Front. Pharmacol.* **2**, 73.

Neher, E., and Sakmann, B. (1976). Single-channel currents recorded from membrane of denervated frog muscle fibres. *Nature* **260**, 799–802.

Neher, E., Sakmann, B., and Steinbach, J. H. (1978). The extracellular patch clamp: A method for resolving currents through individual open channels in biological membranes. *Pflüg. Arch. Eur. J. Physiol.* **375**, 219–228.

Orvos, P., Virág, L., Tálosi, L., Hajdú, Z., Csupor, D., Jedlinszki, N., Szél, T., Varró, A., and Hohmann, J. (2015). Effects of *Chelidonium majus* extracts and major alkaloids on hERG potassium channels and on dog cardiac action potential—a safety approach. *Fitoterapia* **100**, 156–165.

Page, G., Ratchada, P., Miron, Y., Steiner, G., Ghetti, A., Miller, P. E., Reynolds, J. A., Wang, K., Greiter-Wilke, A., Polonchuk, L., *et al.* (2016). Human *ex-vivo* action potential model for pro-arrhythmia risk assessment. *J. Pharmacol. Toxicol. Methods* **81**, 183–195.

Pearlstein, R. A., Vaz, R. J., Kang, J., Chen, X.-L., Preobrazhenskaya, M., Shchekotikhin, A. E., Korolev, A. M., Lysenkova, L. N., Miroshnikova, O. V., Hendrix, J., *et al.* (2003). Characterization of hERG potassium channel inhibition using CoMSiA 3D QSAR and homology modeling approaches. *Bioorg. Med. Chem. Lett.* **13**, 1829–1835.

Perrin, M. J., Kuchel, P. W., Campbell, T. J., and Vandenberg, J. I. (2008). Drug binding to the inactivated state is necessary but not sufficient for high-affinity binding to human ether-a-go-go-related gene channels. *Mol. Pharmacol.* **74**, 1443–1452.

Polonchuk, L. (2012). Toward a new gold standard for early safety: Automated temperature-controlled hERG test on the PatchLiner. *Front. Pharmacol.* **3**, 3.

Qu, Y., Page, G., Abi-Gerges, N., Miller, P. E., Ghetti, A., and Vargas, H. M. (2018). Action potential recording and pro-arrhythmia risk analysis in human ventricular trabeculae. *Front. Physiol.* **8**, 1109.

Roden, D. M. (2008). Repolarization reserve: A moving target. *Circulation* **118**, 981–982.

Roden, D. M., and Yang, T. (2005). Protecting the heart against arrhythmias: Potassium current physiology and repolarization reserve. *Circulation* **112**, 1376–1378.

Rosen, M. R., Wit, A. L., and Hoffman, B. F. (1975). Electrophysiology and pharmacology of cardiac arrhythmias. VI. Cardiac effects of verapamil. *Am. Heart J.* **89**, 665–673.

Sager, P. T., Gintant, G., Turner, J. R., Pettit, S., and Stockbridge, N. (2014). Rechanneling the cardiac proarrhythmia safety paradigm: A meeting report from the Cardiac Safety Research Consortium. *Am. Heart J.* **167**, 292–300.

Salata, J. J., Jurkiewicz, N. K., Wallace, A. A., Stupienski, R. F., Guinosso, P. J., and Lynch, J. J. (1995). Cardiac electrophysiological actions of the histamine H1-receptor antagonists astemizole and terfenadine compared with chlorpheniramine and pyrilamine. *Circ. Res.* **76**, 110–119.

Sale, H., Wang, J., O'Hara, T. J., Tester, D. J., Phartiyal, P., He, J.-Q., Rudy, Y., Ackerman, M. J., and Robertson, G. A. (2008). Physiological properties of hERG 1a/1b heteromeric currents and a hERG 1b-specific mutation associated with Long-QT syndrome. *Circ. Res.* **103**, e81–95.

Sanguinetti, M. C., Jiang, C., Curran, M. E., and Keating, M. T. (1995). A mechanistic link between an inherited and an acquired cardiac arrhythmia: hERG encodes the I_{Kr} potassium channel. *Cell* **81**, 299–307.

Scheel, O., Frech, S., Amuzescu, B., Eisfeld, J., Lin, K. H., and Knott, T. (2014). Action potential characterization of human induced pluripotent stem cell-derived cardiomyocytes using automated patch-clamp technology. *Assay Drug Dev. Technol.* **12**, 457–469.

Trudeau, M. C., Warmke, J. W., Ganetzky, B., and Robertson, G. A. (1995). hERG, a human inward rectifier in the voltage-gated potassium channel family. *Science* **269**, 92–95.

Varró, A., and Baczkó, I. (2011). Cardiac ventricular repolarization reserve: A principle for understanding drug-related proarrhythmic risk. *Br. J. Pharmacol.* **164**, 14–36.

Vormberge, T., Hoffmann, M., and Himmel, H. (2006). Safety pharmacology assessment of drug-induced QT-prolongation in dogs with reduced repolarization reserve. *J. Pharmacol. Toxicol. Methods* **54**, 130–140.

Weerapura, M., Nattel, S., Chartier, D., Caballero, R., and Hébert, T. E. (2002). A comparison of currents carried by hERG, with and without coexpression of MiRP1, and the native rapid delayed rectifier current. Is MiRP1 the missing link? *J. Physiol.* **540**, 15–27.

Windley, M. J., Lee, W., Vandenberg, J. I., and Hill, A. P. (2018). The temperature dependence of kinetics associated with drug block of hERG channels is compound-specific and an important factor for proarrhythmic risk prediction. *Mol. Pharmacol.* **94**, 760–769.

Yap, Y. G., and Camm, A. J. (2003). Drug induced QT prolongation and torsades de pointes. *Heart* **89**, 1363–1372.

Yu, Z., Liu, J., van Veldhoven, J. P., IJzerman, A. P., Schalij, M. J., Pijnappels, D. A., Heitman, L. H., and de Vries, A. A. (2016). Allosteric modulation of Kv11.1 (hERG) channels protects against drug-induced ventricular arrhythmias. *Circ. Arrhythm. Electrophysiol.* **9**, e003439.

Zhang, S., Sawanobori, T., Hirano, Y., and Hiraoka, M. (1997). Multiple modulations of action potential duration by different calcium channel blocking agents in guinea pig ventricular myocytes. *J. Cardiovasc. Pharmacol.* **30**, 489–496.

Zhang, S., Zhou, Z., Gong, Q., Makielski, J. C., and January, C. T. (1999). Mechanism of block and identification of the verapamil binding domain to hERG potassium channels. *Circ. Res.* **84**, 989–998.